

# Raman scattering from the filled tetrahedral semiconductor LiMgN: Identification of the disordered arrangement between Li and Mg

K. Kuriyama,\* Y. Yamashita, and T. Ishikawa

College of Engineering and Research Center of Ion Beam Technology, Hosei University, Koganei, Tokyo 184-8584, Japan

K. Kushida

Department of Arts and Sciences, Osaka Kyoiku University, Osaka 582-8582, Japan

(Received 30 January 2007; published 25 June 2007)

The disordered arrangement between Li and Mg in the filled tetrahedral semiconductor LiMgN, viewed theoretically as a zinc-blende-AlN-like  $(\text{MgN})^-$  lattice partially filled with He-like  $\text{Li}^+$  interstitials, is studied using a Raman-scattering method. A single phonon mode observed at  $492 \text{ cm}^{-1}$  is associated with a  $T_{2g}(\Gamma)$  Raman-active mode as a pure antifluorite structure (space group  $Fm\bar{3}m$ ), indicating the homogeneous random distribution of Li and Mg atoms at the tetrahedral sites. The observed Raman mode is attributed to a vibrational frequency that the randomly occupied Li and Mg atoms vibrate against each other and the N atoms remain stationary. The disordered structure is likely to arise from the relatively high ionic character of Li-N and Mg-N bonds in comparison with Li-P and Mg-P bonds in the ordered filled-tetrahedral semiconductor LiMgP (space group  $F-43m$ ).

DOI: 10.1103/PhysRevB.75.233204

PACS number(s): 78.30.-j, 63.20.-e, 61.66.Fn

The band-structure modification of filled tetrahedral semiconductors was tested by insertion of small atoms at tetrahedral interstitial sites of diamond and zinc-blende structures.<sup>1,2</sup> The crystal structure [Fig. 1(a)] of ordered filled tetrahedral semiconductors  $A^I B^{II} C^V$  such as LiZnN,<sup>3</sup> LiZnP,<sup>4</sup> and LiZnAs<sup>5</sup> is viewed as follows: Whereas the zinc-blende structure of a  $D^{III}-C^V$  compound (e.g., GaN) has the  $D^{III}$  atom at  $\tau_1=(0,0,0)a_0$  (where  $a_0$  is the lattice parameter), the  $C^V$  atom at  $\tau_2=(\frac{1}{4}, \frac{1}{4}, \frac{1}{4})a_0$ , and two empty interstitial sites at  $\tau_3=(\frac{1}{2}, \frac{1}{2}, \frac{1}{2})a_0$  (next to the anion) and  $\tau_4=(\frac{3}{4}, \frac{3}{4}, \frac{3}{4})a_0$  (next to the cation), one could “transmute”  $D^{III}$  into its isovalent pair  $B^{II}-A^I$  (e.g., Ga into Zn+Li) and distribute these atoms among  $\tau_1$ ,  $\tau_2$ , and  $\tau_3$  sites. The  $\tau_1$ ,  $\tau_2$ , and  $\tau_3$  sites for LiZnN are occupied by Zn, N, and Li atoms, respectively, while the  $\tau_4$  site is empty. On the other hand, in ternary compounds<sup>6</sup> such as LiMgN, LiMgP, and LiMgAs, since the ionic radii of  $\text{Li}^+$  and  $\text{Mg}^{2+}$  are approximately equal ( $0.68$  and  $0.66 \text{ \AA}$ ),<sup>6</sup> the conditions are particularly favorable for a random distribution of metals at  $\tau_1$  and  $\tau_3$  sites as shown in Fig. 1(b). In the case of the random distribution, the two sites are not distinguished, and therefore, it can be considered as a virtual cation with average mass between Li and Mg, leading to the space group  $Fm\bar{3}m$  instead of  $F-43m$ . In our previous x-ray diffraction studies of LiMgN,<sup>7</sup> the ordered structure between Li and Mg was not confirmed exactly. However, LiMgP (Ref. 8) crystallizes as the ordered arrangement with Mg at  $\tau_1$  sites and Li at  $\tau_3$  sites rather than the random one. This situation was confirmed by a Raman scattering method because the space group of the ordered LiMgP is  $F-43m$  as well as a zinc-blende structure, showing two longitudinal (LO) and transverse (TO) phonons for Li-P and Mg-P pairs in LiMgP (Ref. 8) as well as LiZnP (Ref. 9) and LiZnAs.<sup>10</sup> For the electronic-structure calculation of the actual LiMgN, it is important to determine whether Li and Mg atoms are the ordered or disordered occupancies, although the band gap<sup>7</sup> of LiMgN has been experimentally evaluated to be  $3.2 \text{ eV}$  at  $300 \text{ K}$ . This gap value is much smaller than that of AlN (zinc

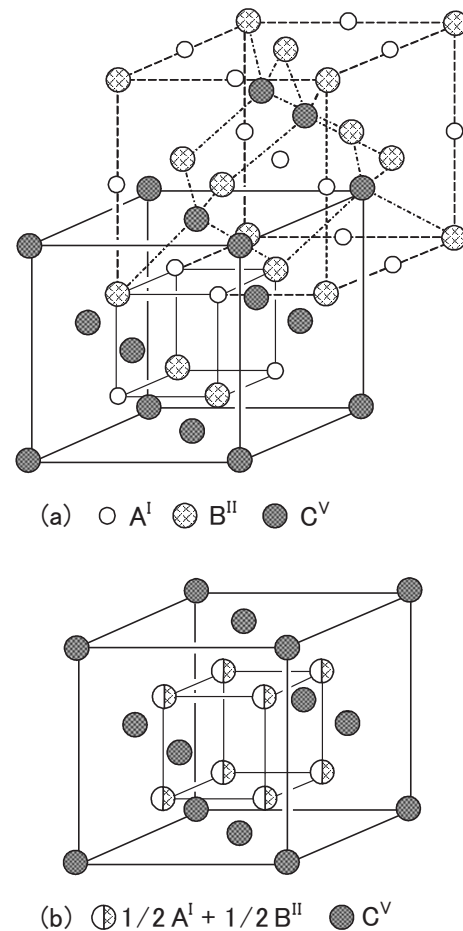


FIG. 1. (a) The ordered filled-tetrahedral structure of  $A^I B^{II} C^V$  ( $A^I=\text{Li}$ ,  $B^{II}=\text{Zn}$  or  $\text{Mg}$ , and  $C^V=\text{N}$ ,  $\text{P}$ , or  $\text{As}$ ; space group  $F-43m$ ) and (b) the disordered structure with homogeneous random distribution of  $A^I$  and  $B^{II}$  metals at the tetrahedral sites. The space group of the disordered phase is  $Fm\bar{3}m$  as well as binary  $\text{Li}_2\text{O}$  antifluorite structure.

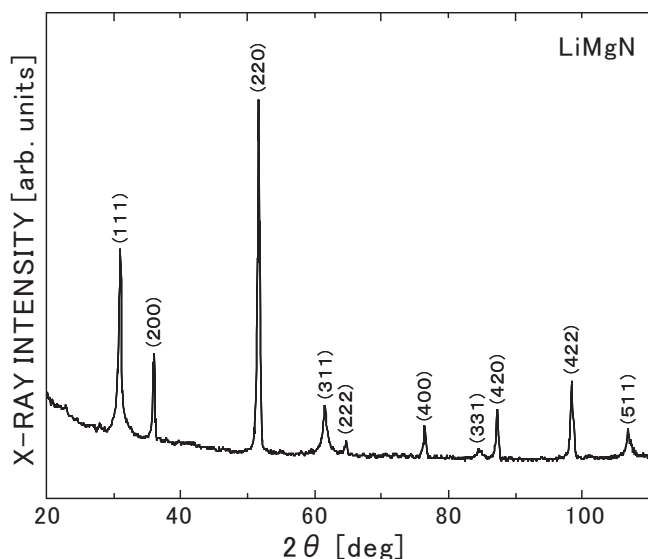


FIG. 2. A typical x-ray powder diffraction pattern of the filled tetrahedral semiconductor LiMgN ( $a=4.995\pm 0.005$  Å).

blende,  $E_g=5.34$  eV),<sup>11</sup> but the value is close to that of GaN (zinc-blende,  $E_g=3.45$  eV).<sup>12</sup> Recent electronic structure calculation<sup>13</sup> of the ordered LiMgN showed an indirect band gap of 2.46 eV.

In this Brief Report we describe the results of Raman scattering from the filled tetrahedral semiconductor LiMgN. We found that an observed Raman-active phonon mode [ $T_{2g}(\Gamma)$ ] attributes to the random distribution of Li and Mg atoms at tetrahedral sites, as a pure antifluorite structure (space group  $Fm\bar{3}m$ ).

Polycrystalline LiMgN samples were synthesized by a direct reaction between  $\text{Li}_3\text{N}$  and Mg in  $\text{N}_2$  atmosphere as well as  $\text{Li}_3\text{AlN}_2$ ,<sup>14</sup> while the previous growth<sup>7</sup> was performed using  $\text{N}_2$  (or  $\text{NH}_3$ ) and LiMg alloy. No Raman scattering data has been obtained from the previous LiMgN samples, although the band gap of LiMgN was evaluated from the previous samples. A present growth method has been performed to improve the sample quality enough to measure the Raman scattering. The detailed growth method will be reported elsewhere. A typical x-ray powder diffraction pattern of as-grown LiMgN polycrystalline is shown in Fig. 2. The present as-grown samples are the single phase with a lattice constant  $a=4.995\pm 0.005$  Å, in contrast with the previous samples including nonreactant LiMg and an oxide ( $\text{LiNO}_3$ ). The reliability indices<sup>15</sup>  $R$  for the disordered and ordered structures were 0.17 and 0.27, respectively. Although the  $R$  indices indicate that the disordered structure is suitable for LiMgN rather than the ordered one, the  $R$  index for the disordered structure is relatively high for the exact determination because of the small atomic scattering factor of Li atom. To compare with a previously reported band gap value,<sup>7</sup> which is taken by a photoacoustic spectroscopy (PAS), the band gap of as-grown LiMgN was measured by the PAS method. The PAS system with a 500 W xenon lamp as a light source was used to detect the PA signal. The signal picked up by a microphone was detected through a lock-in amplifier at room temperature. All the spectra were normalized against a car-

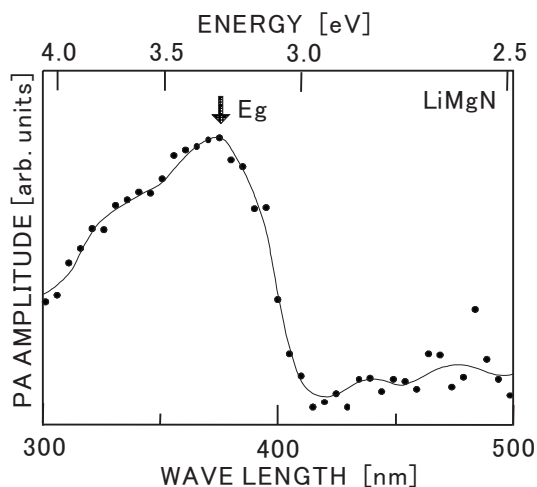


FIG. 3. Photoacoustic emission spectrum taken from as-grown LiMgN.

bon black standard. Figure 3 shows the PAS spectrum for LiMgN. The PA signal begins to increase at photon energy of about 3.0 eV and reaches a peak at around 3.3 eV. Therefore, the band gap is located in 3.3 eV, which is close to the previously reported value (3.2 eV).<sup>7</sup>

A laser Raman spectrophotometer (JASCO NR-1800) was employed for a study on Raman scattering. The Raman spectra were taken at room temperature in backscattering geometry using a 514.5 nm line of  $\text{Ar}^+$ -ion gas laser with a power of 100 mW. Cross sections of cracked polycrystalline LiMgN samples, protected by paraffin oil to prevent rapid oxidation and hydration, were used for the Raman measurements.

Figure 4 shows a typical Raman spectrum of LiMgN. A single frequency mode was observed at  $492\text{ cm}^{-1}$ , which is analogous to antifluorite  $\text{Li}_2\text{O}$ <sup>16</sup> (space group  $Fm\bar{3}m$ ) that also showed a single Raman active phonon mode  $T_{2g}(\Gamma)$  at  $520\text{ cm}^{-1}$ . From factor group analysis for the ordered and disordered phase of LiMgN,  $2F_2$  modes are Raman active for the ordered filled tetrahedral structure ( $F\bar{4}3m$ ) and  $T_{2g}$  mode

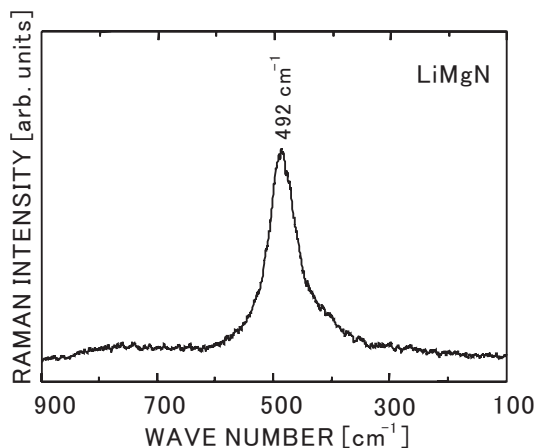


FIG. 4. A typical Raman spectrum of the filled tetrahedral semiconductor LiMgN.

is Raman active for the disordered phase with homogeneously random distribution of Li and Mg. Any orientation effect on the Raman scattering would be eliminated, since the samples used here were polycrystalline. In the case of the ordered structure, two Raman peaks corresponding to the TO and LO modes can be observed from each pair of Li-N and Mg-N, as observed in LiZnP (Ref. 9) and LiZnAs.<sup>10</sup> Contrary, if the samples belong to the  $Fm\bar{3}m$  point group, the crystal is centrosymmetric and no long range electrical field exists. Therefore, there is no TO-LO splitting and just the nonpolar  $T_{2g}$  Raman active mode can be observed. Accordingly, the mode observed in LiMgN would originate to the antifluorite structure ( $Fm\bar{3}m$ ) with a random occupation of Li and Mg atoms at the tetrahedral positions  $\tau_1$  and  $\tau_3$  sites in Fig. 1. The other evidence of the disorder distribution is a broader linewidth of  $35\text{ cm}^{-1}$  for the Raman spectrum. This situation has been observed in mixed-fluorite-type crystals<sup>17</sup>  $\text{Ca}_x\text{Sr}_{1-x}\text{F}_2$  and  $\text{Sr}_x\text{Ba}_{1-x}\text{F}_2$  in which the linewidths of Raman spectra were maximum at homogeneous random mixtures with a composition of  $x=0.5$ . Since the arrangement that changed cation and anion of fluorite  $\text{CaF}_2$ -type structure is antifluorite-type structure, the broader Raman spectrum observed here suggests homogeneous random arrangements of Li and Mg. By simply assuming the so-called “virtual-crystal” approximation<sup>18</sup> and from the analogy of ionic motion in mixed-fluorite-type crystals<sup>17</sup>  $\text{Ca}_x\text{Sr}_{1-x}\text{F}_2$ , the Li+Mg cations having average masses vibrate against each other and the N anion remains stationary in analogy to the vibration modes in antifluorite  $\text{Li}_2\text{O}$  crystal,<sup>16</sup> which have a single allowed Raman-active mode in which the  $\text{Li}^+$  ions vibrate against each other and the  $\text{O}^{2-}$  ion remains stationary.

Finally we discuss why LiMgN crystallizes in the disordered structure ( $Fm\bar{3}m$ ) in contrast to other filled tetrahedral compounds ( $F\bar{4}3m$ ). We pay attention to a difference in Pauling’s ionicity of Li-X and Mg-X (Zn-X) in LiMgX (LiZnX) compounds, where X is N, P, or As. According to Pauling,<sup>19</sup> the definition of ionicity of a single bond is as follows:

$$f_i = 1 - \exp[-(X_A - X_B)^2/4], \quad (1)$$

where  $X_A$  and  $X_B$  are Pauling’s electronegativity of A and B elements, respectively. Assuming that the above equation is

TABLE I. Pauling’s bond ionicity ( $f_i$ ) in the filled tetrahedral compounds.

X	LiMgX		LiZnX	
	$f_i(\text{Li-X})$	$f_i(\text{Mg-X})$	$f_i(\text{Li-X})$	$f_i(\text{Zn-X})$
N	0.63	0.55	0.63	0.39
P	0.26	0.18	0.26	0.06
As	0.22	0.15	0.22	0.04

valid for ternary compounds, the ionicity ( $f_i$ ) values for LiMgX and LiZnX are evaluated as listed in Table I. The crystal structure of the compounds listed in Table I has been exactly confirmed by x-ray diffraction analysis, except for LiMgN and LiMgAs. The  $f_i$  values for Li-N bond (0.63) and Mg-N (0.55) in LiMgN all exceed 0.5, indicating that both bonds have high ionicity. This is consistent with the results estimated from the density functional theory-based electronic structure calculation<sup>20</sup> of LiMgN as follows. The bonding nature is due to the large electronegativity difference between N and Mg, and Li behaves effectively as  $\text{Li}^+$  ions. On the other hand, in the other filled tetrahedral compounds, the  $f_i$  values of Li-X and Mg-X (Zn-X) bonds are relatively low ( $f_i < 0.5$ ) except for that of Li-N in LiZnN. These results suggest that both Li-X and Mg-X (Zn-X) bonds in LiMgX (LiZnX) are required to possess high ionicity in order to form the disordered antifluorite structure. Therefore, LiMgP would crystallize in the ordered structure because of the  $f_i$  values ( $f_i < 0.5$ ) of Li-P and Mg-P in spite of the almost same ionic radii<sup>6</sup> of  $\text{Li}^+$  and  $\text{Mg}^{2+}$ .

In conclusion, the disordered structure of Li and Mg atoms in the filled tetrahedral semiconductor LiMgN was studied using a Raman-scattering method. A single allowed Raman-active mode [ $T_{2g}(\Gamma)$ ] was observed as well as a pure antifluorite structure (space group  $Fm\bar{3}m$ ), showing the homogeneous random distribution of Li and Mg atoms at the tetrahedral sites. It is suggested that the disordered structure attributes to the high ionic character of both Li-N and Mg-N bonds.

\*kuri@ionbeam.hosei.ac.jp

<sup>1</sup>D. M. Wood, A. Zunger, and R. de Groot, Phys. Rev. B **31**, 2570 (1985).

<sup>2</sup>A. E. Carlsson, A. Zunger, and D. M. Wood, Phys. Rev. B **32**, 1386 (1985).

<sup>3</sup>K. Kuriyama, T. Kato, and T. Tanaka, Phys. Rev. B **49**, 4511 (1994).

<sup>4</sup>R. Bacewicz and T. F. Ciszek, Appl. Phys. Lett. **52**, 1150 (1988); K. Kuriyama and T. Katoh, Phys. Rev. B **37**, 7140 (1988).

<sup>5</sup>K. Kuriyama, T. Kato, and K. Kawada, Phys. Rev. B **49**, 11452 (1994).

<sup>6</sup>R. Juza, K. Langer, and K. von Benda, Angew. Chem., Int. Ed. Engl. **7**, 360 (1968).

<sup>7</sup>K. Kuriyama, K. Nagasawa, and K. Kushida, J. Cryst. Growth **237/239**, 2019 (2002).

<sup>8</sup>K. Kuriyama, K. Kushida, and R. Taguchi, Solid State Commun. **112**, 429 (1998).

<sup>9</sup>K. Kuriyama, Y. Takahashi, and K. Tomizawa, Phys. Rev. B **47**, 13861 (1993).

<sup>10</sup>K. Kuriyama, T. Ishikawa, and K. Kushida, Phys. Rev. B **72**, 233201 (2005).

<sup>11</sup>M. P. Thompson, G. W. Auner, T. S. Zheleva, K. A. Jones, S. J. Steven, and J. N. Hilfiker, J. Appl. Phys. **89**, 3331 (2001).

<sup>12</sup>J. Petalas, S. Logothetidis, S. Boultaidakis, M. Alouani, and J. M. Wills, Phys. Rev. B **52**, 8082 (1995).

<sup>13</sup>F. Kalarasse, B. Bennecer, and A. Mellouki, J. Phys.: Condens.

- Matter **18**, 7237 (2006).
- <sup>14</sup>K. Kushida, Y. Kaneko, and K. Kuriyama, Phys. Rev. B **70**, 233303 (2005); K. Kuriyama, Y. Kaneko, and K. Kushida, J. Cryst. Growth **275**, e395 (2005).
- <sup>15</sup>J. Donohue and K. N. Trueblood, J. Appl. Crystallogr. **9**, 615 (1956).
- <sup>16</sup>K. Kunc, I. Loa, A. Grzechnik, and K. Syassen, Phys. Status Solidi B **242**, 1857 (2005).
- <sup>17</sup>R. K. Chang, B. Lacina, and P. S. Pershan, Phys. Rev. Lett. **17**, 755 (1966).
- <sup>18</sup>I. Nair and C. T. Walker, Phys. Rev. B **3**, 3446 (1971), and references therein.
- <sup>19</sup>L. Pauling, *The Nature of the Chemical Bond*, 3rd ed. (Cornell University Press, Ithaca, New York, 1960), p. 91.
- <sup>20</sup>H. C. Kandpal, C. Felser, and R. Seshadri, J. Phys. D **39**, 776 (2006).